Journal of Pharmaceutical Analysis 10 (2020) 13–22

Contents lists available at ScienceDirect

Journal of Pharmaceutical Analysis

journal homepage: www.elsevier.com/locate/jpa

Original Article

Karacoline, identified by network pharmacology, reduces degradation of the extracellular matrix in intervertebral disc degeneration via the NF-κB signaling pathway

Xiaoli Zhou [a], Yingying Hong [b], Yulin Zhan [c, *]

[a] Department of Traditional Chinese Medicine, College of Medicine, Shanghai University of Traditional Chinese Medicine, Shanghai, 201203, China
[b] Department of Biology, School of Fisheries and Life Sciences, Shanghai Ocean University, Shanghai, 201306, China
[c] Orthopedics Department, Shanghai Sixth People's Hospital East Affiliated to Shanghai University of Medicine&Health Science, Shanghai, 201306, China

ARTICLE INFO

Article history:
Received 3 February 2019
Received in revised form
17 July 2019
Accepted 19 July 2019
Available online 26 July 2019

Keywords:
Karacoline
Network pharmacology
Intervertebral disc degeneration
Extracellular matrix
Matrix metalloproteinases

ABSTRACT

Karacoline is a compound found in the plant *Aconitum kusnezoffii* Reichb. Although *Aconitum kusnezoffii* Reichb is widely used for the treatment of pain, very few studies have been carried out on the use of karacoline due to its potential toxicity. In this study, we selected key matrix metalloproteinases (MMPs), collagen II, and aggrecan as targets due to their association with intervertebral disc degeneration (IDD). Using these targets, we then used network pharmacology to predict a series of molecules that might exert therapeutic effects on IDD. Of these molecules, karacoline was predicted to have the best effect. Tumor necrosis factor (TNF)-α is known to promote the degeneration of the extracellular matrix in IDD. We therefore applied different concentrations of karacoline (0, 1.25, or 12.88 μM) along with 100 ng/mL TNF-α to rat nucleus pulposus cells and found that karacoline reduced the expression of MMP-14 in IDD by inhibiting the nuclear factor (NF)-κB pathway, while collagen II and aggrecan expression was increased. This suggested that extracellular matrix degradation was inhibited by karacoline ($P < 0.05$). Our data therefore reveal a new clinical application of karacoline and provide support for the use of network pharmacology in predicting novel drugs.

1. Introduction

Low back pain is an extremely common and frequently chronic disease. Indeed, according to a 2017 survey on the global burden of 354 diseases, low back pain was ranked in the top place in terms of the number of years that patients live with disability [1]. Many studies have suggested that low back pain is closely related to intervertebral disc degeneration (IDD) [2]. Although the precise mechanism underlying IDD is not fully understood, it is very apparent that degradation of the extracellular matrix (ECM) in the nucleus pulposus is one of the major characteristic changes. The main components of the ECM are collagen II and aggrecan. Collectively, these components allow the nucleus pulposus to retain water and therefore buffer and absorb pressure. In a healthy disc, the synthesis and decomposition of the ECM are in equilibrium, predominantly due to the complex regulation of growth factors and catabolic cytokines. When the catabolic activity of the ECM exceeds its anabolic activity, there is a reduction in the relative content of collagen II and aggrecan, leading to water loss and the development of IDD [3]. Previous research has shown that tumor necrosis factor (TNF)-α promotes degradation of the ECM, and may initiate the initial production of matrix metalloproteinases (MMPs) [4].

MMPs are the main enzymes for degrading collagen and aggrecan. Higher expression levels of MMPs can be detected in degenerative intervertebral discs compared to normal discs [5]. One previous study in humans analyzed the relationship between different IDD grades and MMP-1 expression, and the results showed that MMP-1 expression was up-regulated with increasing degenerative grade [6]. Another study found up-regulated levels of MMP-2 in degenerative intervertebral discs after comparing the gene expression profiles of normal and degenerative intervertebral discs [7]. However, the MMP-3 gene can be expressed at high levels

Peer review under responsibility of Xi'an Jiaotong University.
* Corresponding author.
E-mail address: sd_zhanyl@sumhs.edu.cn (Y. Zhan).

https://doi.org/10.1016/j.jpha.2019.07.002

in degenerative intervertebral disc tissues in response to a wide range of different factors [8]. LeMaitre et al. [9] further showed that the expression of MMP-7 in chondrocyte-like cells of the nucleus pulposus increased with the aggravation of degeneration at the histological level. MMP-7 can degrade the major matrix molecules of the intervertebral disc, which is accompanied by the activation of many other proteases and cytokines, and it plays an important role in the degeneration of intervertebral discs. Although the levels of MMP-8 were shown not to be significantly up-regulated in degenerative IDD, MMP-8 expression gradually increased as the level of degeneration increased [10]. High MMP-10 expression has also been detected in the tissues of patients with symptomatic disc degeneration, which might represent the beginning of pain perception [11]. Other research has shown that MMP-12 is not only involved in degradation of the ECM in IDD but is also related to the activity of both cytokines and chemokines [12]. Li et al. [13] subsequently showed a positive correlation between levels of MMP-13 in degenerative intervertebral disc tissues and the degree of degeneration. In another study, Xu et al. [14] reported that while there was no significant difference in the expression of MMP-14 in intervertebral discs when compared between individuals of different ages, MMP-14 expression increased as the degree of degeneration increased. Most recently, Zhang et al. [15] showed that MMP-16 can degrade aggrecan and collagen II, thus leading to water loss and disc degeneration. Given the potential of MMP-14 as a marker for predicting IDD [16], we adopted this molecule as our main target in the experiments conducted as part of this study.

Currently, the treatment of IDD in clinical practice is still based on symptomatic therapies for single symptoms. While surgical treatment can be performed if the disease worsens, there remains no effective method to reverse or even delay the disease process. The precise regulation of specific biological targets may reverse the degradation of the ECM in IDD. Network pharmacology is a research method based on high-throughput omics analysis, use of interaction network databases, and virtual computing; this technique can be used to identify new drugs and determine the mechanistic actions of drugs. Network pharmacology analyzes the relationships between drugs and diseases in a systematic manner, and thus reveals the mechanisms of drugs acting upon the human body and allows us to predict new drugs with therapeutic effects from a database of compounds [17]. Two key databases can be used in network pharmacology. The first is the Connectivity Map Database, which contains the gene expression profiles of human cells in response to a large number of biologically active small molecules. The database can match a gene expression phenotype that is of interest to the user to microarray data on more than 1,300 small molecules. The output is a list of compounds with scores that represent correlations with the gene expression phenotype. These correlations range from high positive correlations (indicating similarity to the gene expression phenotype provided by the user) to high negative correlations (indicating the reverse of the gene expression phenotype provided by the user). Thus, a negative score may indicate a therapeutic effect [18]. The second database is the Traditional Chinese Medicine Systems Pharmacology (TCMSP) database, which features approximately 30,000 active molecules that can be found in Chinese herbal medicines. This database features important data on absorption, distribution, metabolism, and excretion (ADME)-related properties such as oral bioavailability, drug-likeness, and the half-life associated with oral administration in humans [19].

In this study, we selected key genes that are known to be related to ECM degradation during IDD as potential regulatory targets. We then used a combination of network pharmacology and the concept of "disease-target-component-drug" to identify (using the Connectivity Map Database) potential therapeutic molecules for experimental validation and database screening (using the TCMSP database). In addition, we screened for the potential therapeutic molecules that can be sourced from traditional Chinese medicines, in the hope of laying a foundation for the exploration of combination therapy involving traditional Chinese medicine in the future.

2. Materials and methods

2.1. Target selection and drug screening

First, we identified members of the MMP family that are specifically up-regulated in IDD (MMP-1, -2, -3, -7, -8, -10, -12, -13, -14 and -16), and collagen II and aggrecan, which are both down-regulated in IDD, as specific drug targets. All of them were selected by searching the literature. A human protein interaction network was obtained from the Human Protein Reference Database, and Cytoscape 3.6.1 software (NRNB, CA, USA) was used to establish a protein interaction network. The Connectivity Map Database [18] was used to compare the gene expression profile of the disease (IDD) with the gene expression profiles of human cells in response to biologically active small molecules. The database allowed us to predict the effects of the molecules (in terms of their effects on human cells' gene expression profile) and obtain Connectivity Map scores for them. Molecules with negatives scores were used as candidate therapeutic molecules, meaning that they were screened for in the TCMSP database [19] to identify molecules that can be sourced from Chinese herbal medicines. Given that oral bioavailability (OB) and drug-likeness (DL) are important indicators to assess the feasibility of using a molecule as a therapeutic drug, we established preset criteria ($OB \geq 30.0$ and $DL \geq 0.18$) to screen for the molecules in the TCMSP.

2.2. Reagents and antibodies

Karacoline (PLC≥98% by high-performance liquid chromatography [HPLC]) was purchased from Shanghai Chengshao Biological (Shanghai, China). Anti-nuclear factor (NF)-κB p65 (acetyl K310) antibody and anti—NF—κB p65 (phospho S536) antibody were purchased from Abcam (Cambridge, MA, USA) while other antibodies were purchased from SAB (Baltimore, MD, USA). RPMI 1640 medium and fetal bovine serum (FBS) were purchased from BBI (Markham, CA, USA). Recombinant rat TNF-α was purchased from Sangon Biotech (Shanghai, China). Rat MMP-14 ELISA Kit, Rat Col II ELISA Kit and Rat Aggrecan ELISA Kit were purchased from Enzyme-linked Biotechnology (Shanghai, China).

2.3. Cell culture and identification

Primary culture nucleus pulposus cells, obtained from Sprague-Dawley rats, were purchased from Rochen Pharma Co., Ltd. (Shanghai, China). These cells were cultured at 37 °C in 5% CO_2, and then grown to 90% confluence. The 3,3-diaminobenzidine (DAB) method was used to identify nucleus pulposus cells. Slides of nucleus pulposus cells were prepared and fixed with 4% paraformaldehyde fix solution (BBI), sealed with goat serum (BBI), and incubated overnight at 4 °C with anti-collagen II rabbit antibody (diluted 1:200, SAB). The primary antibody was then washed off and horseradish peroxidase (HRP)-conjugated goat anti-rabbit IgG (BBI) was added, and the cells were incubated at room temperature

for 1 h. DAB was used for color development, and hematoxylin was used as a counterstain. Finally, neutral balsam mounting medium was used to seal the slides, which were then observed under an inverted microscope (Olympus Corporation, Tokyo, Japan). The nucleus pulposus cells of rats with collagen II positive rate >90% were used for the experiments.

2.4. Cell counting kit 8 (CCK8)

Approximately 5×10^3 nucleus pulposus cells were placed into each well of a 96-well cell culture plate with complete medium (90% RPMI 1640 medium and 10% FBS), exposed to different concentrations of karacoline (0.001, 0.010, 0.10, 1.0, 10.0, 100.0 and 1000.0 μM), and incubated for 24 h. The medium was then removed and replaced with 100 μL complete medium and 10 μL CCK8 solution; the cells were then incubated at 37 °C for 2 h. A blank group (complete medium only) and a control group (complete medium and nucleus pulposus cells) were prepared at the same time. The optical density (OD) at 450 nm was then determined using a microplate reader (BioTek Instruments Inc., Winooski, VT, USA). Cell survival rate was then calculated according to the following formula: Cell viability (%) = (OD treatment group-OD blank group)/(OD control group-OD blank group). The half maximal inhibitory concentration (IC50) value of karacoline regarding nucleus pulposus cells was calculated, and then the maximum dose without cytotoxicity was calculated. In addition, after adding different concentrations of TNF-α (50, 100, and 150 ng/mL), which promotes the degeneration of nucleus pulposus cells, cytotoxicity was detected at different time points (days 0, 1, 2, and 3) using the methodology described above.

2.5. Real-time quantitative polymerase chain reaction (RT-qPCR)

Nucleus pulposus cells were incubated for 24 h with different concentrations of karacoline and 100 ng/mL TNF-α. Next, 1 mL total RNA extractor (Sangon Biotech) was used to lyse the cells, followed by incubation at room temperature for 10 min. Thereafter, 200 μL chloroform was added and the cells were mixed with a vortexer for 15 s. They were then allowed to rest at room temperature for 3min, and then centrifuged at 12,000×*g* and 4 °C for 10 min. The upper water phase was placed into a clean centrifuge tube and the same amount of isopropanol was added. The samples were left at room temperature for 20 min and then centrifuged at 12,000×*g* and 4 °C for 10 min. The supernatant was then discarded and 1 mL 75% ethanol was added to cause precipitation. The samples were then centrifuged again at 12,000×*g* and 4 °C for 20 min and the supernatant was removed. The samples were then dried at room temperature for 5–10 min and 30–50 μL RNase-free ddH_2O was used to fully dissolve the resultant RNA.

The RNA was transcribed into complementary DNA using Super Moloney Murine Leukemia Virus (M-MuLV) Reverse Transcriptase (Diamond) and reverse transcription primers for the target genes (MMP-14, COL2A1 [which encodes collagen II], and ACAN [which encodes aggrecan]). Transcription was carried out at 50 °C for 30 min, then 80 °C for 15 min, followed by a cooling phase on ice. RT-qPCR was then performed by an MX3000P Real-Time Fluorescence Quantitative PCR System (Strata-gene, USA) using the following protocol: denaturation at 95 °C for 3 min and then 40 cycles of 95 °C for 12 s and 62 °C for 40 s. Glyceraldehyde 3-phosphate dehydrogenase (GAPDH) was used as an internal control. Primers for the amplification of target genes were designed and then pairs of primers were selected using BLAST in PubMed (Table 1).

Table 1
Sequences of the primers used for qPCR.

Gene name	Primer sequences
MMP14	F:5′-ATGGAAGCAAGTCAGGGTCA-3′ R:5′-ACCATCGCTCCTTGAAGACA-3′
COL2A1	F:5′-CTCATCCAGGGCTCCAATGA-3′ R:5′- CCATGGGTGCAATGTCAACA-3′
ACAN	F:5′- GTTATCGCCACTTTCCCGAC-3′ R:5′- ATTGCAGGGAGTGTCCATCA-3′
GAPDH	F:5′-ACCACAGTCCATGCCATCAC-3′ R:5′-TCCACCACCCTGTTGCTGTA-3′

qPCR = Quantitative polymerase chain reaction; MMP14 = Matrix metalloproteinase 14; GAPDH = Glyceraldehyde-3-phosphate dehydrogenase.

2.6. Enzyme-linked immunosorbent assay (ELISA)

ELISAs were performed using Rat MMP-14, Col II, and AGG ELISA Kits (Enzyme-linked Biotechnology, Shanghai, China). Nucleus pulposus cells were treated with different concentrations of karacoline (0, 1.25, or 12.88 μM) and 100 ng/mL TNF-α in complete medium (90% RPMI 1640 medium and 10% FBS) for 48 h. The mixture was then centrifuged at 300×*g* for 20 min, and the supernatant was collected. Next, 50 μL of standard substance at concentrations of 32, 16, 8, 4, 2, and 1 ng/mL were added to a microtiter plate. Thereafter, 50 μL of each supernatant was added to other wells. With the exception of wells that were left as blanks, 100 μL HRP labeled detection antibody was added to each of the wells (containing the standards or supernatants). The plates were then sealed with film and incubated at 37 °C for 60 min. The liquid in each well was then discarded and the plate was patted dry with absorbent paper. Each well was then filled with wash solution and allowed to stand for 1 min. The liquid was then discarded and the plate was patted dry with absorbent paper. This procedure was repeated five times. Next, 50 μL substrate A and 50 μL substrate B were added to each well and incubated in the dark at 37 °C for 15 min. Thereafter, 50 μL stop solution was added to each well and the OD at 450 nm was determined (within 15 min) with a microplate reader (BioTek Instruments Inc., Winooski, VT, USA). To create a standard curve and obtain a linear regression equation, OD values were plotted on the x-axis and the concentration of the standard substance was plotted on the y-axis. The OD values of the supernatants were substituted into the equation to calculate the protein concentrations of MMP-14, collagen II, and aggrecan.

2.7. Western blotting

To investigate proteins that are characteristic indicators of NF-κB pathway activation (p65, phospho-p65, and acetylated-p65), nucleus pulposus cells were treated with different concentrations of karacoline (0, 1.25, or 12.88 μM) and 100 ng/mL TNF-α for 24 h. To investigate the protein levels of MMP-14, collagen II, and aggrecan, different concentrations of karacoline (0, 1.25, or 12.88 μM) and 100 ng/mL TNF-α were added for 48 h. A Tissue or Cell Total Protein Extraction Kit (Sangon Biotech) was then used to extract total cell protein, and 10% sodium dodecyl sulfate polyacrylamide gel electrophoresis (SDS-PAGE) was used to separate 20 μL total protein per well. After electrophoresis, the separated proteins were transferred to a polyvinylidene fluoride (PVDF) membrane and incubated overnight with the following primary antibodies: anti-aggrecan antibody (1:1000, SAB), anti-collagen II antibody (1:1000, SAB), anti-MMP-14 antibody (1:1000, SAB), anti–NF–κB p65 mouse

monoclonal antibody (1:1000, SAB), anti–NF–κB p65 (phospho S536) antibody (1:1000, Abcam), and anti–NF–κB p65 (acetyl K310) antibody (1:1000, Abcam). On the following day, the membranes were treated with HRP-conjugated goat anti-rabbit IgG (1:2000, Jackson, PA, USA), and chemiluminescence was assessed using SuperSignal West Pico Chemiluminescent Substrates (Pierce, WDC, USA). Finally, the membranes were exposed to X-ray films and the resultant films were photographed with the X-Omat BT Film (Kodak, NY, USA). Protein quantification was then performed with a Gel-Pro Analyzer 4.0 (Media Cybernetics, WDC, USA), and bands with a positive response were quantified by densitometry and normalized against GAPDH.

2.8. Immunofluorescence

Microscope slides were placed in a 12-well cell culture plate and nucleus pulposus cells were placed on the slides at a density of 2×10^4/mL. The next day, the cells were treated with 100 ng/mL

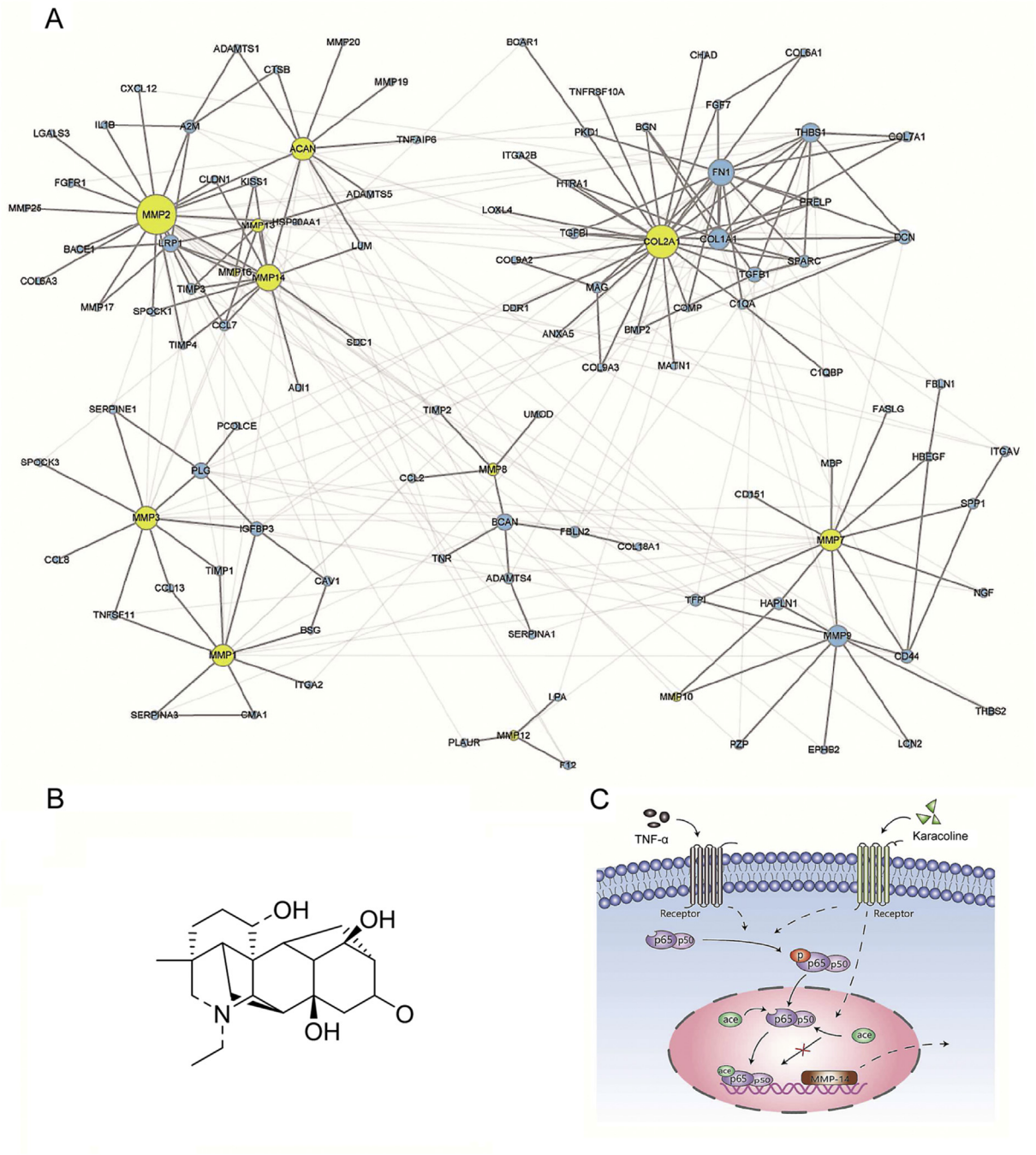

Fig. 1. (A) Protein interaction network of MMPs, collagen II and aggrecan. The size of each dot indicates how much it interacts with other proteins. (B) Molecular formula of karaoline. (C) Effect of karaoline on TNF-α-induced NF-κB signaling pathway activation.

TNF-α, 100 ng/mL TNF-α + 1.25 μM karacoline, or 100 ng/mL TNF-α + 12.88 μM karacoline. The slides were removed 4 days later and fixed with 4% paraformaldehyde for 15 min. The cells were treated with 0.5% Triton X-100 at room temperature for 20 min and then incubated with goat serum at room temperature for 1 h. The cells were then treated with anti-aggrecan antibody (1:200, SAB), anti-collagen II antibody (1:200, SAB), and anti-MMP-14 antibody (1:200, SAB) at 4 °C overnight. The cells were then incubated for 1 h at 37 °C with DyLight 549 goat anti-rabbit IgG antibody (Vector Laboratories, CA, USA) and then incubated with 4,6-diamidino-2-phenylindole (DAPI; BBI) for 5 min in the dark to stain the nuclei. The cells were then washed with phosphate-buffered saline plus Tween 20 (PBST; Sangon Biotech) and then dried. A sealing agent, containing a fluorescence quenching agent, was then applied and the images were observed and quantified under a fluorescence microscope.

2.9. Flow cytometry

Apoptosis was assessed using an Annexin V-Fluorescein Isothiocyanate (FITC) Apoptosis Detection Kit (BBI). Nucleus pulposus cells were added to a 6-well culture plate at a density of 5×10^4/mL and were then treated with the highest dose of karacoline without cytotoxicity (as demonstrated in a previous experiment) or twice the IC50 dose of karacoline (also determined in a previous experiment) combined with 100 ng/mL TNF-α for 48 h. The cells were then washed with phosphate-buffered saline (PBS) and centrifuged at 300×*g* for 5 min. The supernatant was then discarded and the cells were resuspended in 195 μL 1 × binding buffer to obtain a cell density of 5×10^5/mL. Next, 5 μL annexin V-FITC was added and incubated at room temperature in the dark for 10 min. Subsequently, 1 × binding buffer was used to wash the cells, which were then centrifuged at 300×*g* for 5 min; the supernatant was discarded. Finally, the cells were resuspended in 190 μL 1 × binding buffer, and 10 μL propidium iodide was added to stain the nuclei red. Samples were immediately analyzed by flow cytometry (BD Biosciences, San Jose, CA, USA), each sample counts 1×10^4 cells.

2.10. Statistical analysis

Quantity One (Bio-Rad Laboratories, CA, USA) was used for the grayscale analysis of the Western blotting results. GraphPad Prism 8 (GraphPad Software, CA, USA) was used for all other data analyses. Student's *t*-test was used for all pairwise comparisons, and differences were considered to be statistically significant if $P < 0.05$.

Table 2
Top 10 molecules that were identified using the Connectivity Map Database and then ranked by Connectivity Map score.

Molecule	Connectivity Map score	OB (%)	DL
Karakoline	−0.841	51.73	0.73
Tetrahydroalstonine	−0.775	32.42	0.81
Boldine	−0.702	31.18	0.51
Lysergol	−0.675	48.11	0.27
Papaverine	−0.652	64.04	0.38
Fisetin	−0.606	52.6	0.24
Lobelanidine	−0.577	60.53	0.32
Artemisinin	−0.572	49.88	0.31
Noscapine	−0.567	53.29	0.88
Podophyllotoxin	−0.536	59.94	0.86

OB = Oral bioavailability; DL = Drug-likeness.

3. Results

3.1. Targets and drugs for IDD

Compared with normal intervertebral discs, degenerative intervertebral discs exhibit greater expression levels of MMPs and lower expression levels of collagen II and aggrecan. These targets are central markers of IDD, and multiple proteins interact with them. Consequently, a protein interaction network can be obtained (Fig. 1A). In the network diagram, the size of each dot indicates the degree of protein interaction, so we can deduce that COL2A1 (which encodes collagen II), ACAN (which encodes aggrecan), and MMP-14 show high levels of probable interaction. Using the Connectivity Map and TCMSP databases, 15 molecules were identified and ranked by their Connectivity Map scores. The top 10 molecules are given in Table 2. Karacoline, which was ranked first in the list of 10 molecules, was selected for subsequent experimental verification (Fig. 1B). Given the role of TNF-α in IDD, and the fact that it can activate the NF-κB pathway to stimulate the secretion of MMP-14, karacoline was combined with TNF-α to verify whether karacoline could reverse the effects of TNF-α (Fig. 1C). The nucleus pulposus cells of rats with collagen II positive rate >90% were used for the experiments (Fig. 2A).

3.2. Effects of karacoline and TNF-α on the viability of nucleus pulposus cells

Our data showed that the high dose of karacoline was cytotoxic to nucleus pulposus cells. CCK8 assays were used to detect the cell viability of nucleus pulposus cells under different concentrations of karacoline. The IC50 was calculated to be 6.444 μM (Fig. 2B). The maximum dose of karacoline without cytotoxicity to nucleus pulposus cells was calculated to be 1.25 μM. Using TNF-α at different concentrations, the CCK8 assay was performed again. The results demonstrated that 1.25 μM karacoline antagonized the toxic effect of TNF-α on nucleus pulposus cells to some extent (Fig. 2C).

3.3. Karacoline reversed the expression of genes induced by TNF-α

Nucleus pulposus cells were treated with 0, 1.25, or 12.88 μM of karacoline and 100 ng/mL TNF-α, and qPCR was then performed. The data showed that TNF-α significantly up-regulated the expression of the MMP-14 gene, and down-regulated the expression of collagen II and aggrecan. Interestingly, karacoline reversed this effect. Both 1.25 and 12.88 μM karacoline led to inhibition of MMP-14 gene expression, while the gene encoding collagen II was up-regulated ($P < 0.05$, Figs. 2D and F). Additionally, 1.25 μM of karacoline increased the expression of aggrecan ($P < 0.05$, Fig. 2E).

3.4. Karacoline inhibited TNF-α-induced ECM degradation

Considering that ECM degradation is a key feature of IDD, we used a variety of methods to investigate the mechanisms involved. The outer surfaces of nucleus pulposus cells were treated with 100 ng/mL TNF-α with different concentrations of karacoline (0, 1.25, or 12.88 μM), and the culture supernatant was then analyzed by ELISA. The results showed that TNF-α significantly decreased the secretion of collagen II and aggrecan in the supernatant. This situation was reversed by treatment with karacoline. Both 1.25 and 12.88 μM karacoline increased the content of aggrecan in the supernatant, while 1.25 μM karacoline also increased collagen II ($P < 0.05$, Figs. 3A and B). We also used western blotting to measure the intracellular content of collagen II and aggrecan proteins. Unfortunately, there were no statistically significant differences ($P < 0.05$, Figs. 3D and E). The immunofluorescence experiments

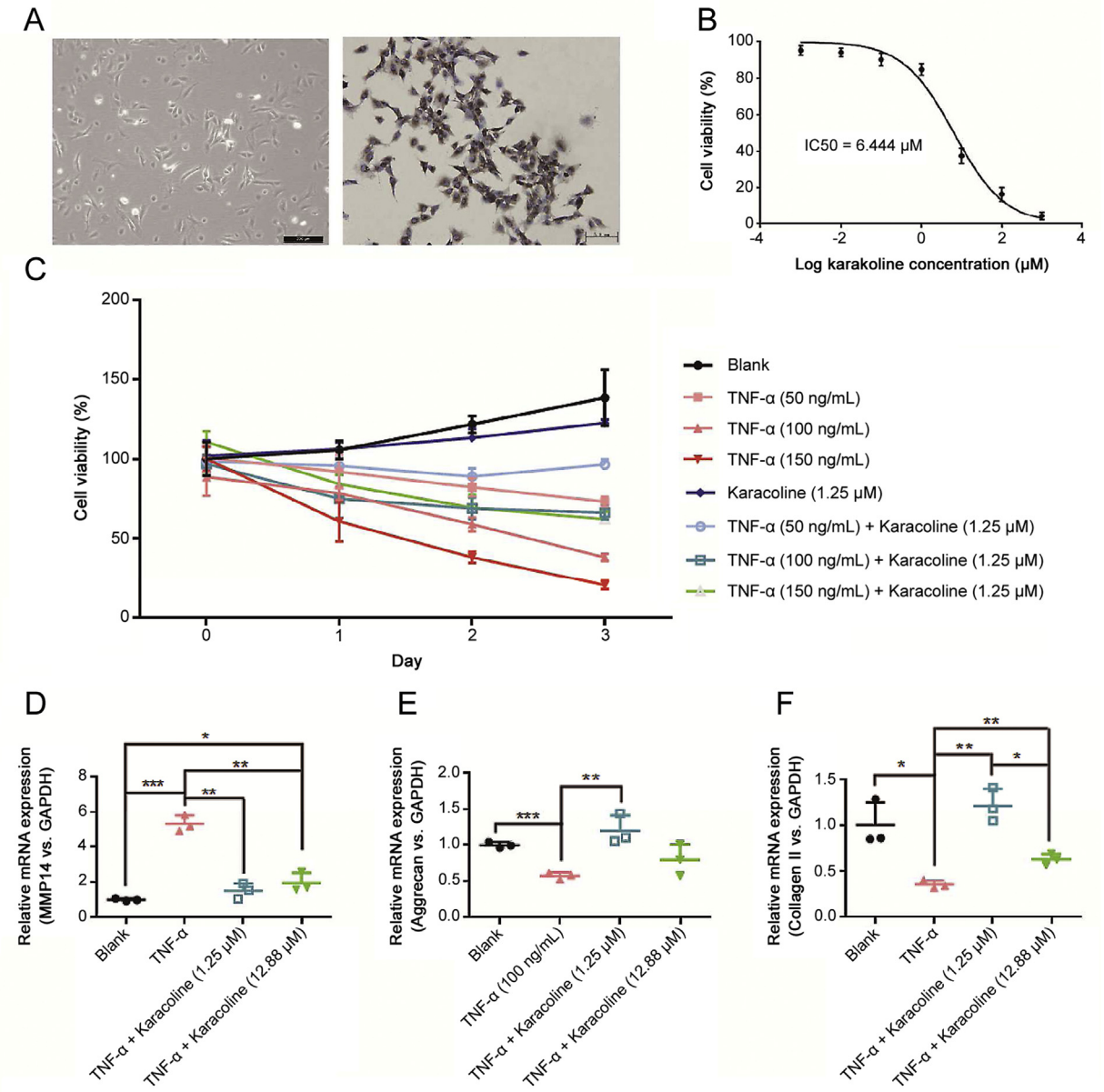

Fig. 2. (A) Immunohistochemical identification of rat nucleus pulposus cells. (B) Half maximal inhibitory concentration (IC50) of karacoline. (C) Cytotoxicity of karacoline at different concentrations of TNF-α. (D, E, F) Expression of MMP-14, aggrecan, and collagen II in rat nucleus pulposus cells treated with 0, 1.25, or 12.88 μM karacoline and 100 ng/mL TNF-α (*$P < 0.05$, **$P < 0.01$, ***$P < 0.001$).

clearly showed that compared with the TNF-α-only group, karacoline significantly increased the content of aggrecan and collagen II in the nucleus pulposus cells (Figs. 3F and G).

3.5. Karacoline inhibited TNF-α-induced NF-κB pathway activation and thereby reduced MMP-14 secretion

ELISA of culture supernatants indicated that 100 ng/mL TNF-α significantly increased the secretion of MMP-14 while the concentration of MMP-14 in the supernatant was reduced by 1.25 μM karacoline ($P < 0.05$, Fig. 3C). Western blotting also confirmed that the expression of the MMP-14 protein in nucleus pulposus cells was significantly increased by the addition of 100 ng/mL TNF-α, but it was significantly reduced by 1.25 μM karacoline ($P < 0.05$, Figs. 3D and E). The same findings were also evident in our immunofluorescence data, which showed that when only 100 ng/mL TNF-α was added, the distribution of MMP-14 in nucleus pulposus cells increased, but this was decreased with the addition of 1.25, or 12.88 μM karacoline (Fig. 3H). TNF-α can activate the NF-κB pathway to stimulate the secretion of MMP-14, so we hypothesized that karacoline could inhibit this effect. The levels of acetylated-p65 (characteristic indicators of NF-κB pathway activation) was increased when only 100 ng/mL TNF-α was added, but both 1.25 and 12.88 μM karacoline could curb these effects. However, there was no significant difference in the levels of phospho-p65 between each group, suggesting that the NF-κB pathway was inhibited by karacoline, especially through its negative effects on p65 acetylation ($P < 0.05$, Figs. 3D and E).

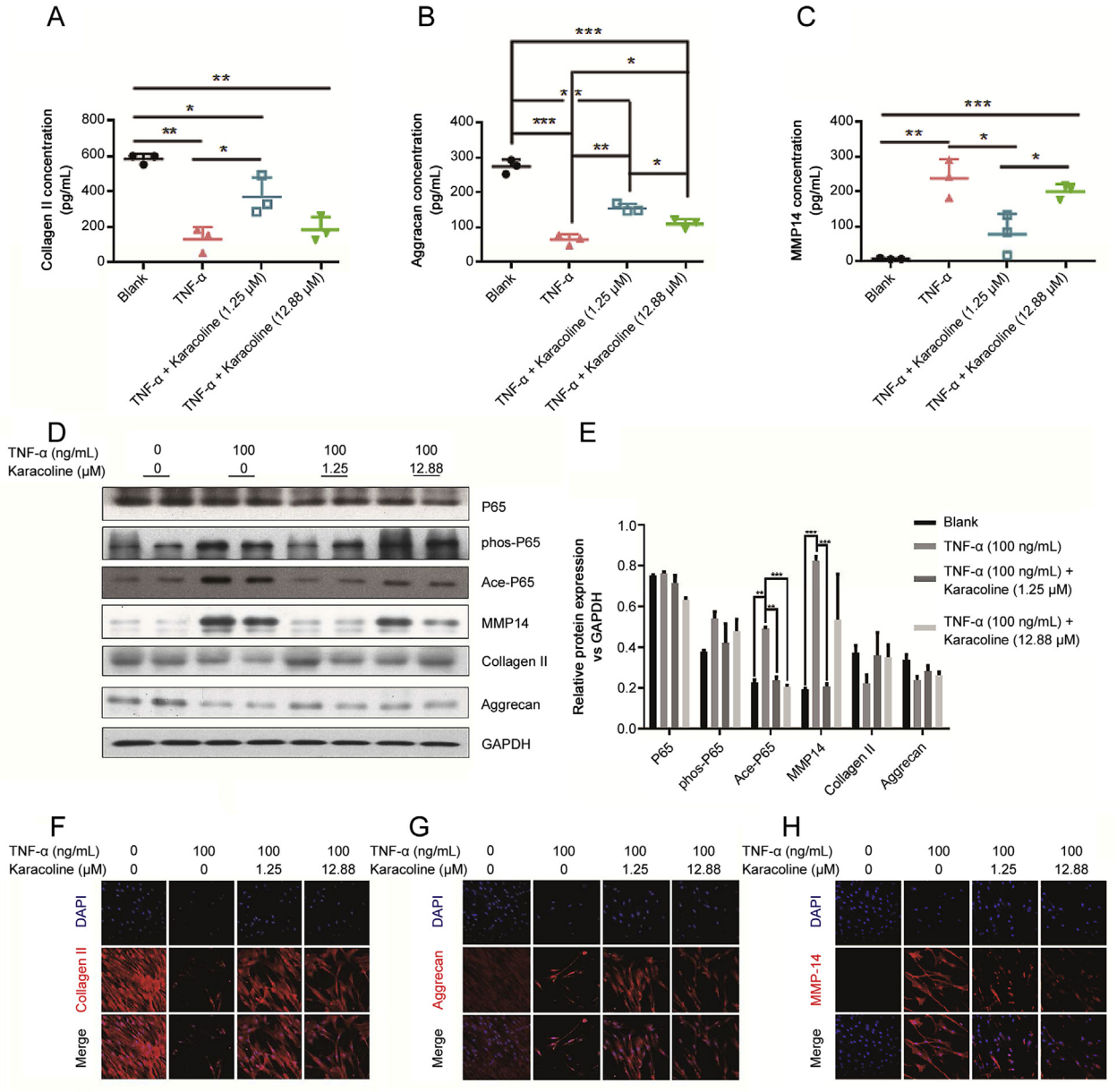

Fig. 3. (A, B, C) Secretion of collagen II, aggrecan, and MMP-14 in culture supernatant with 0, 1.25, or 12.88 μM karacoline and 100 ng/mL TNF-α (*$P < 0.05$, **$P < 0.01$, ***$P < 0.001$). (D) Western blotting results showing levels of phospho-p65, acetylated-p65, MMP-14, collagen II, and aggrecan in nucleus pulposus cells treated with 0, 1.25, or 12.88 μM karacoline and 100 ng/mL TNF-α. (E) Column analysis diagram of Western blotting results (*$P < 0.05$, **$P < 0.01$, ***$P < 0.001$). (F, G, H) Immunofluorescence of rat nucleus pulposus cells treated with 0, 1.25, or 12.88 μM karacoline and 100 ng/mL TNF-α.

3.6. Anti-apoptosis effect of karacoline on nucleus pulposus cells treated with TNF-α

A high concentration of karacoline was cytotoxic to nucleus pulposus cells, while TNF-α induced apoptosis of nucleus pulposus cells. Both 1.25 and 12.88 μM karacoline antagonized TNF-α-induced apoptosis (Fig. 4).

4. Discussion

The health and economic burden of IDD is significant. As such, a wide body of research has been carried out to investigate the factors that lead to the degradation of the ECM. Via these studies, the roles of many individual molecules have been elucidated. For example, one study showed that streptozotocin-induced diabetic mice had disc degeneration and high expression levels of MMP-13 but also that a combined treatment of pentosan polysulfate and pyridoxine alleviated disc degeneration by reducing the expression of MMP-13 [20]. In another study, a specific inhibitor of NF-κB, BAY11-7082, was administered to human nucleus pulposus cells exposed to interleukin (IL)-1; the results showed that the gene expression of MMP-3, MMP-9, and MMP-13 were decreased, and also that the low expression of aggrecan and collagen II was reversed [21]. These studies confirmed the associations between MMPs, aggrecan, and collagen II. Our current study is the first to investigate the specific role of karacoline in IDD.

Karacoline is a natural herbal extract, which is mainly found in *Aconitum kusnezoffii* Reichb (a traditional Chinese herbal medicine).

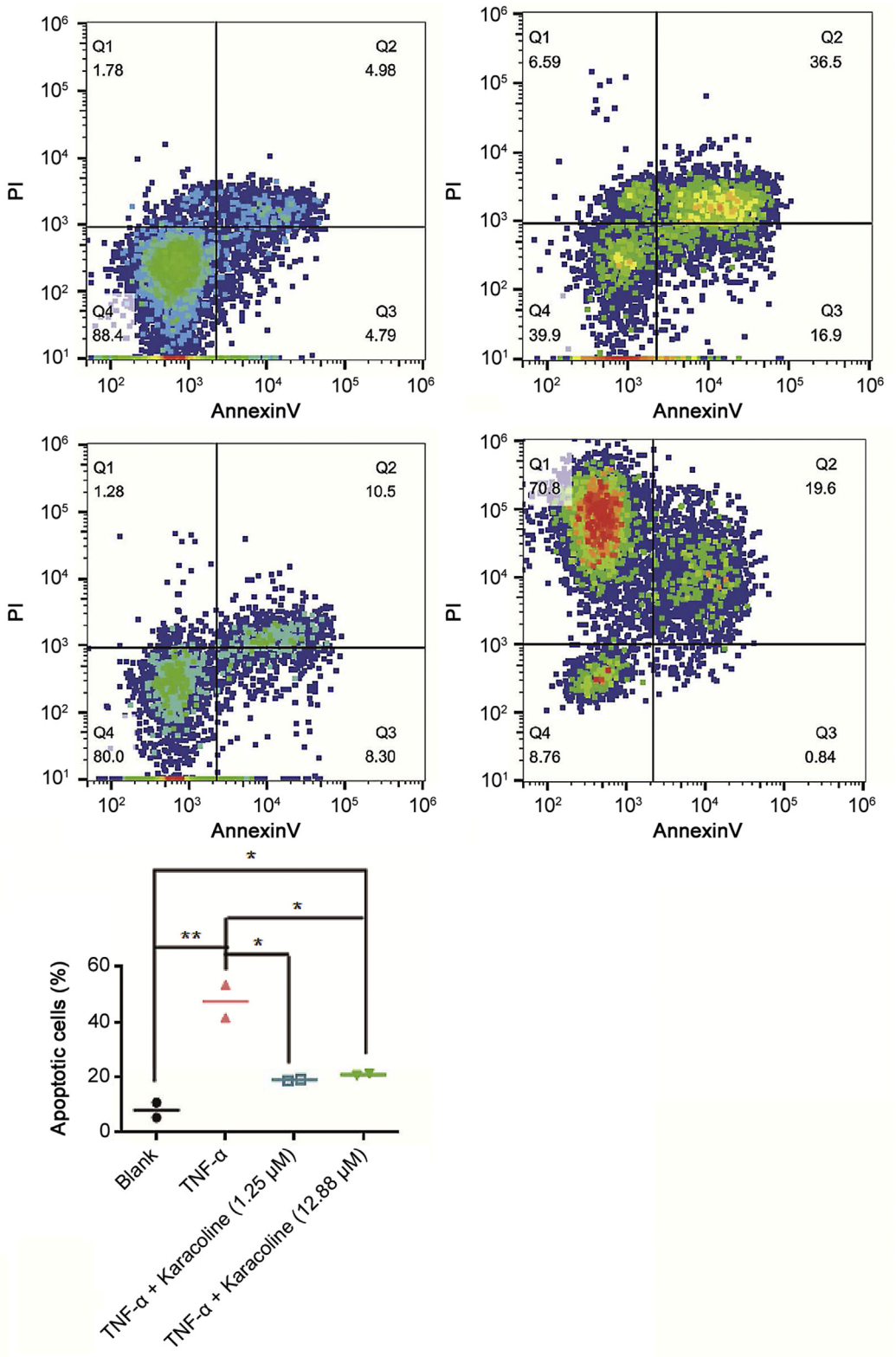

Fig. 4. Karacoline reduced TNF-α-induced apoptosis in rat nucleus pulposus cells.

The clinical application of *Aconitum kusnezoffii* Reichb has previously been limited because of its potential toxicity. However, due to its powerful analgesic effect, it is still widely used in the treatment of diseases associated with pain symptoms. The efficacy of this medicine is remarkable, and the key to its rational use is identifying the balance between efficacy and safety [22]. Similarly, the administration of karacoline must involve an appropriate dose. Our experiments showed that a low dose of karacoline was better than a high dose. In our experiment, we showed that karacoline effectively inhibited the activation of the NF-κB pathway and thereby reduced the production of MMP-14; this significantly reduced the degradation of the ECM.

Prior to this study, the potential role of karacoline in disease treatment had not been investigated; researchers have generally ignored this medicine because of its toxicity. Our analyses were innovative in this sense, because we initially used network pharmacology predictions to identify the potential role of karacoline in IDD treatment. Interestingly, our network predictions showed that karacoline was not the only important drug, as multiple other molecules were identified that are also worth exploring. This is not the first time that network pharmacology has been used to screen for drugs that could be used for the treatment of specific diseases. In terms of Western medicine compounds, a previous study compared the gene expression profiles of 100 diseases with the gene expression profiles in response to 164 drug compounds, which yielded predictions regarding their therapeutic potentials, many of which were shown to have entirely new indications. For example, an anti-ulcer drug, cimetidine, was predicted to be a candidate therapeutic agent for lung adenocarcinoma; this prediction was confirmed in vitro and in vivo using a mouse xenotransplantation model [23]. At present, the application of network pharmacology in Chinese herbal medicine is more focused on the further exploration of known medical compounds that can influence disease-related targets. For example, the plant-based combination therapy "*Astragalus-Angelica*" is used to treat traumatic brain injury; the target for this Chinese herbal medicine was first predicted by network pharmacology, and the accuracy of this prediction was then verified experimentally [24].

As described above, the value of this study lies not only in the discovery of single compounds, but also in the fact that multiple of these compounds can be mapped to traditional Chinese medicine combinations to create multi-target treatments. In fact, multi-target treatment is not a new concept. In the field of acquired immune deficiency syndrome (AIDS) treatment, combinations of drugs have been shown to be highly effective. For example, Atripla is marketed as a "cocktail therapy" for HIV infection and is composed of three drugs: efavirenz, emtricitabine, and tenofovir disoproxil fumarate. It remains a commonly used treatment for AIDS because it is tolerated well by patients and exhibits excellent efficacy [25]. In the field of cancer therapy, the combination of palbociclib and letrozole significantly increases the anti-tumor activity of palbociclib [26]. This demonstrates the advantage of multi-target combination therapy, which is an inherent strategy in traditional Chinese medicine. We can see that a single compound can exhibit good effects, but if multiple therapeutic compounds can be sourced from Chinese herbal medicine and administered as combination therapy, the efficacy may be much higher, which will be a key focus of our future research.

Acknowledgments

This work was supported by the Pudong New Area Science and Technology Committee of Shanghai (Grant No. PKJ2015-Y08).

Conflicts of interest

The authors declare that there are no conflicts of interest.

Appendix A. Supplementary data

Supplementary data to this article can be found online at https://doi.org/10.1016/j.jpha.2019.07.002.

References

[1] S.L. James, D. Abate, K.H. Abate, et al., Global, regional, and national incidence, prevalence, and years lived with disability for 354 diseases and injuries for 195 countries and territories, 1990-2017: a systematic analysis for the Global Burden of Disease Study 2017, Lancet 392 (2018) 1789–1858.
[2] K. Luoma, H. Riihimäki, R. Luukkonen, et al., Low back pain in relation to lumbar disc degeneration, Spine 25 (2000) 487–492.
[3] A.M. Wang, P. Cao, A. Yee, et al., Detection of extracellular matrix degradation in intervertebral disc degeneration by diffusion magnetic resonance spectroscopy, Magn. Reson. Med. 73 (2015) 1703–1712.
[4] C. Wang, X. Yu, Y. Yan, et al., Tumor necrosis factor-α: a key contributor to intervertebral disc degeneration, Acta Biochim. Biophys. Sin. 49 (2017) 1–13.
[5] N.V. Vo, R.A. Hartman, T. Yurube, et al., Expression and regulation of metalloproteinases and their inhibitors in intervertebral disc aging and degeneration, Spine J. 13 (2013) 331–341.
[6] H. Xu, Q. Mei, J. He, et al., Correlation of matrix metalloproteinases-1 and tissue inhibitor of metalloproteinases-1 with patient age and grade of lumbar disk herniation, Cell Biochem. Biophys. 69 (2014) 439–444.
[7] Y. Tang, S. Wang, Y. Liu, et al., Microarray analysis of genes and gene functions in disc degeneration, Exp. Ther. Med. 7 (2014) 343–348.
[8] H.V. Yuan, Y. Tang, Y.X. Liang, et al., Matrix metalloproteinase-3 and vitamin d receptor genetic polymorphisms, and their interactions with occupational exposure in lumbar disc degeneration, J. Occup. Health 52 (2010) 23–30.
[9] C.L. LeMaitre, A.J. Freemont, J.A. Hoyland, Human disc degeneration is associated with increased MMP 7 expression, Biotech. Histochem. 81 (2006) 4–6.
[10] B. Bachmeier, A. Nerlich, N. Mittermaier, et al., Matrix metalloproteinase expression levels suggest distinct enzyme roles during lumbar disc herniation and degeneration, Eur. Spine J. 18 (2009) 1573–1586.
[11] S.M. Richardson, P. Doyle, B.M. Minogue, et al., Increased expression of matrix metalloproteinase-10, nerve growth factor and substance p in the painful degenerate intervertebral disc, Arthritis Res. Ther. 11 (2009) R216.
[12] H.E. Gruber, J.A. Ingram, M.D. Cox, et al., Matrix metalloproteinase-12 immunolocalization in the degenerating human intervertebral disc and sand rat spine: biologic implications, Exp. Mol. Pathol. 97 (2014) 1–5.
[13] H.R. Li, Q. Cui, Z.Y. Dong, et al., Downregulation of miR-27b is Involved in Loss of Type II collagen by directly targeting matrix metalloproteinase 13 (MMP13) in human intervertebral disc degeneration, Spine 41 (2016) E116–E123.
[14] H. Xu, Q. Mei, B. Xu, et al., Expression of matrix metalloproteinases is positively related to the severity of disc degeneration and growing age in the east Asian lumbar disc herniation patients, Cell Biochem. Biophys. 70 (2014) 1219–1225.
[15] W.L. Zhang, Y.F. Chen, H.Z. Meng, et al., Role of miR-155 in the regulation of MMP-16 expression in intervertebral disc degeneration, J. Orthop. Res. 35 (2017) 1323–1334.
[16] J. Zhang, X. Sun, J. Liu, et al., The role of matrix metalloproteinase 14 polymorphisms in susceptibility to intervertebral disc degeneration in the Chinese Han population, Arch. Med. Sci. 11 (2015) 801–806.
[17] B. Chen, A.J. Butte, Network medicine in disease analysis and therapeutics, Clin. Pharmacol. Ther. 94 (2013) 627–629.
[18] J. Lamb, E.D. Crawford, D. Peck, et al., The Connectivity Map: using gene-expression signatures to connect small molecules, genes, and disease, Science 313 (2006) 1929–1935.
[19] J. Ru, P. Li, J. Wang, et al., TCMSP: a database of systems pharmacology for drug discovery from herbal medicines, J. Cheminf. 6 (2014) 13, https://doi.org/10.1186/1758-2946-6-13.
[20] S. Illien-Junger, F. Grosjean, D.M. Laudier, et al., Combined anti-inflammatory and anti-age drug treatments have a protective effect on intervertebral discs in mice with diabetes, PLoS One 8 (2013), e64302.
[21] Z. Sun, S. Zhao, C. Liu, et al., Effects of nuclear factor kappa B signaling pathway in human intervertebral disc degeneration, Spine 40 (2015) 224–232.
[22] Z. Sui, Q. Li, L. Zhu, et al., An integrative investigation of the toxicity of *Aconiti kusnezoffii* radix and the attenuation effect of its processed drug using a UHPLC-Q-TOF based rat serum and urine metabolomics strategy, J. Pharm. Biomed. Anal. 145 (2017) 240–247.
[23] M. Sirota, J.T. Dudley, J. Kim, et al., Discovery and preclinical validation of drug indications using compendia of public gene expression data, Sci. Transl. Med.

3 (2011) 96ra77.
[24] G. Xie, W. Peng, P. Li, et al., A network pharmacology analysis to explore the effect of on traumatic brain injury, BioMed Res. Int. 2018 (2018) 3951783.
[25] E. Deeks, C. Perry, Efavirenz/emtricitabine/tenofovir disoproxil fumarate single-tablet regimen (Atripla®): a review of its use in the management of HIV infection, Drugs 70 (2010) 2315–2338.
[26] B. Warth, P. Raffeiner, A. Granados, et al., Metabolomics reveals that dietary xenoestrogens alter cellular metabolism induced by palbociclib/letrozole combination cancer therapy, Cell. Chem. Biol. 25 (2018) 1–10.